RESEARCH ARTICLE

Value of GCET1, HGAL (GCET2), and LMO2 in the Determination of Germinal Center Phenotype in Diffuse Large B-cell Lymphoma

Diffüz Büyük B-Hücreli Lenfomada Germinal Merkez Fenotipinin Belirlenmesinde GCET1, HGAL (GCET2) ve LMO2'nin Değeri

Neslihan Berker[1], Gülçin Yeğen[1], Yasemin Özlük[1], Öner Doğan[1,2]

[1]İstanbul University İstanbul Faculty of Medicine, Department of Pathology, İstanbul, Türkiye
[2]Koç University Faculty of Medicine, Department of Pathology, İstanbul, Türkiye

Abstract

Objective: Diffuse large B-cell lymphoma (DLBCL) is a biologically heterogeneous disease that is classified into germinal center B-cell (GCB) and non-GCB subtypes, which are prognostically different. The Hans algorithm is the most widely used tool based on CD10, BCL6, and MUM1 expression, but some cases with the non-GCB phenotype are still known to be misclassified. In this study, we investigate the extent to which GCET1, HGAL, and LMO2 protein expressions reflect GCB phenotype together with their roles in determining the GCB phenotype of DLBCL and their contributions to the performance of the Hans algorithm.

Materials and Methods: Sixty-five cases of DLBCL-not otherwise specified, 40 cases of follicular lymphoma (FL), and 19 non-GC-derived lymphoma cases were included in this study. The DLBCL cases were grouped as CD10$^+$ (Group A) or only MUM1$^+$ (Group B), and the remaining cases constituted the intermediate group (Group C). GCET1, HGAL, and LMO2 expressions were evaluated.

Results: In the FL group, GCET1, HGAL, and LMO2 were positive in 85%, 77.5%, and 100% of the cases, respectively. Among the non-GC-derived lymphoma cases, all three markers were negative in cases of small lymphocytic lymphoma, plasmablastic lymphoma, peripheral T-cell lymphoma, and anaplastic large cell lymphoma. GCET1 and HGAL were negative in cases of marginal zone lymphoma (MZL) and mantle cell lymphoma (MCL). Two of the 3 MZL and 2 of the 4 MCL cases were positive for LMO2. In the DLBCL group, the number of cases with GCET1, HGAL, and LMO2 positivity was 18 (90%), 17 (85%), and 20 (100%), respectively, in Group A and 0 (0%), 2 (13.3%), and 2 (13.3%), respectively, in Group B. Considering these rates, when the cases in the intermediate group were evaluated, it was concluded that 13 cases typed as non-GCB according to the Hans algorithm may have the GCB phenotype.

Conclusion: GCET1, HGAL, and LMO2 are highly sensitive markers for determining the germinal center cell phenotype and can increase the accuracy of the subclassification of DLBCL cases, especially for cases that are negative for CD10.

Keywords: Diffuse large B-cell lymphoma, Immunohistochemistry, GCET1, GCET2 (HGAL), LMO2, Hans algorithm

Öz

Amaç: Diffüz büyük B-hücreli lenfoma (DBBHL), germinal merkez B (GMB) hücre ve non-GMB hücre olmak üzere prognostik olarak farklı alt grupları olan biyolojik olarak heterojen bir hastalıktır. CD10, BCL6 ve MUM1 ekspresyonuna göre yapılan Hans algoritması ile GMB olgularının bazıları yanlış sınıflandırılmaktadır. Çalışmamızda, immünohistokimyasal olarak GMB hücre belirteçleri olan GCET1, HGAL ve LMO2'nin folikül merkez hücre fenotipini ne derecede yansıttığını, DBBHL'de GMB hücre fenotipini belirlemedeki rolünü ve Hans algoritmasına katkısını araştırmaktayız.

Gereç ve Yöntemler: Altmış beş adet DBBHL-NOS, 40 adet foliküler lenfoma (FL) ve 19 adet non-GM kökenli lenfoma olgusu çalışmaya alındı. DBBHL olguları CD10$^+$ (Grup A), sadece MUM1$^+$ (Grup B) ve kalanlar ara grup (Grup C) olarak gruplandı. GCET1, HGAL ve LMO2 ekspresyonları değerlendirildi.

Bulgular: FL grubunda, GCET1, HGAL ve LMO2 sırasıyla %85, %77,5, %100 olguda pozitif saptandı. Küçük lenfositik lenfoma, plazmablastik lenfoma, periferik T-hücreli lenfoma ve anaplastik büyük hücreli lenfoma olgularında 3 antikor da negatifti. Marjinal zon lenfoma (MZL) ve mantle hücreli lenfoma (MHL) olgularında GCET1 ve HGAL negatifken; LMO2, 2 MZL ve 2 MHL'de pozitif bulundu. DBBHL olgularında, Grup A'da GCET1, HGAL and LMO2 pozitif olgu sayısı sırasıyla 18 (%90), 17 (%85), 20 (%100) iken, Grup B'de sırasıyla 0 (%0), 2 (%13,3), 2 (%13,3) idi (p<0,001). Bu oranlar göz önüne alınarak ara gruptaki olgular değerlendirildiğinde, Hans algoritmasına göre non-GMB olarak tiplendirilen 13 olgunun GMB fenotipli olabileceği sonucuna varıldı.

Sonuç: GCET1, HGAL ve LMO2, GMB fenotipini belirlemede duyarlı belirteçler olup, DBBHL'lerin (özellikle CD10 negatif olguların) doğru tiplendirilmesine katkı sağladıkları düşünülmüştür.

Anahtar Sözcükler: Diffüz büyük B-hücreli lenfoma, İmmünohistokimya, GCET1, GCET2 (HGAL), LMO2, Hans algoritması

Introduction

Diffuse large B-cell lymphoma (DLBCL) is a mature B-cell neoplasm accounting for 40% of all non-Hodgkin lymphomas. Most of these patients respond to chemotherapy, but fewer than 50% of them can be cured [1,2]. The International Prognostic Index (IPI), which is based on clinical parameters, has been used to assess the risk profiles of patients [3]. However, because of differences in survival among patients with the same IPI scores, there are ongoing efforts to discover new molecules that may allow the identification of the subtypes of DLBCL and develop targeted therapies. Gene expression profiling (GEP) has been performed to investigate the relationship between the molecular characteristics of DLBCL and prognosis [4,5,6,7]. In such studies, DLBCL cases are divided into the three molecular subgroups of germinal center (GC) B-like (GCB), activated B-like (ABC), and type 3 (unclassified) [4,5,7]. Patients treated with cyclophosphamide, doxorubicin, vincristine, and prednisone (CHOP) or other CHOP-like treatment regimens were shown to have better survival independently of their IPI scores among patients with GCB-like DLBCL [3,4,5]. New genetic classifications of DLBCL consisting of various genetic alterations showing different outcomes were also recently described [8,9,10,11].

As GEP studies and molecular analyses are expensive and cannot be applied routinely worldwide, immunohistochemical methods were also developed for target molecules [12,13,14,15,16,17,18]. Among these methods, an algorithm including CD10, BCL6, and MUM1 antibodies, known as the Hans algorithm, was the first algorithm to investigate the correlation between gene expression profiles and antigen expressions. It is the most widely used algorithm for determining the molecular subtypes of DLBCL. However, although the majority of the cases diagnosed in this way correlate well with the GEP profile, some cases categorized into the ABC subgroup with the Hans algorithm are found to be misclassified [12].

GEP studies have shown that the GC expressed transcript 1 (*GCET1*), human germinal center-associated lymphoma (*HGAL*), and LIM domain only 2 (*LMO2*) genes were highly expressed in GC lymphocytes and GC-derived lymphomas, whereas they were not expressed in activated peripheral blood B-cells [4,5,19,20]. New algorithms including GCET1 and LMO2 antibodies have been reported to have higher correlations with GEP results than the Hans algorithm [15,17,18].

In this study, we aim to evaluate the additive value of GCET1, HGAL, and LMO2 in the determination of GCB phenotypes in DLBCL-not otherwise specified (NOS) cases, and especially for triple-negative or CD10$^-$MUM1$^+$BCL6$^+$ cases.

Materials and Methods

Case Selection

In order to investigate the extent to which GCET1, HGAL, and LMO2 antigen expressions reflect GCB phenotype, we retrieved samples from 59 lymphoma cases for the control group, consisting of 40 nodal follicular lymphoma (FL) cases (20 high-grade/grade 3 and 20 low-grade/grade 1-2 cases) and 19 non-GC-derived lymphoma cases including 4 mantle cell lymphoma (MCL), 3 marginal zone lymphoma (MZL), 5 small lymphocytic lymphoma (SLL), 3 plasmablastic lymphoma (PBL), 2 peripheral T-cell lymphoma (PTCL), and 2 anaplastic large-cell lymphoma (ALCL) cases. A total of 65 DLBCL-NOS cases diagnosed between 2010 and 2016 were also included in the study. A standard immunohistochemical panel including CD3, CD20, CD10, BCL6, MUM1, BCL2, CD5, CD23, C-myc, and EBER in situ hybridization was applied for all of the DLBCL-NOS cases. Twenty-five of them were classified as being of the GCB phenotype and 40 of them as the non-GCB phenotype according to the Hans algorithm [12] (Figure 1). Extranodal cases, cases that had transformed from low-grade lymphoma, and cases with accompanying HIV positivity were excluded.

We reviewed all of the archived glass slides, revised the diagnoses according to the 2022 classification of the World Health Organization [21], and determined the morphological subgroups as follows: centroblast-dominant (centroblast ratio of >50%), immunoblast-dominant (immunoblast ratio of >50%), and anaplastic. We also reevaluated the CD10, BCL6, and MUM1 expressions from the archive slides.

Besides the outputs of the Hans algorithm, we created new subgroups. Based on the reliability of CD10 positivity in reflecting GCB phenotypes, the CD10-positive cases were defined as Group A, MUM1-positive cases (CD10$^-$BCL6$^-$) as Group B, and all remaining cases not included in the aforementioned groups as Group C (intermediate group, with triple-negative or only BCL6$^+$ or BCL6$^+$MUM1$^+$ cases as the majority of misclassified cases are of these types) [12,18].

Immunohistochemical Analysis

Immunohistochemical studies were performed using sections of formalin-fixed paraffin-embedded tissues representing the tumor, each 2-3 µm in thickness, with an automated
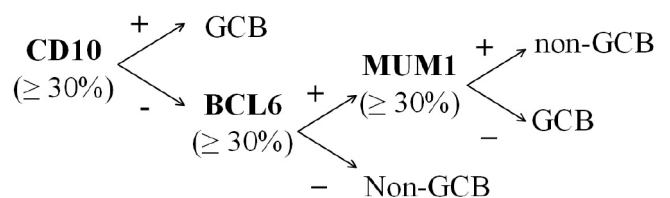

Figure 1. Hans algorithm.

immunostainer (Benchmark XT/ISH Staining Module, Ventana Medical Systems, Oro Valley, AZ, USA). Details regarding antibodies, sources, clones, pretreatments, and dilutions are summarized in Table 1. Palatine tonsil tissue was used as a positive control. Cytoplasmic staining of GCB cells was accepted as positive for GCET1 and HGAL, and nuclear staining of GCB cells and endothelial cells was accepted as positive for LMO2.

Immunohistochemical Evaluation and Hierarchical Clustering

For all cases, the percentage of positively stained cells was calculated. Based on percentages of positive staining for all three antibodies in Groups A and B, receiver operating characteristic curve analysis was used to obtain cut-off values for differentiating the GCB and non-GCB phenotypes (Figure 2). These cut-off point values were calculated using the Youden index (Y = sensitivity + specificity - 1), as this method can be applied to find optimal cut-off values with the highest sensitivity and specificity when there is no particular requirement for sensitivity and/or specificity. The calculated cut-off values used to define the immunoreactivity as positive were ≥30% for GCET1, ≥20% for HGAL, and ≥50% for LMO2.

The Cluster 3.0 and Treeview 3.0 programs were used for hierarchical clustering to integrate and visualize all immunohistological staining results for the DLBCL cases, as described previously by Eisen et al. [22]. This method was used previously in the literature for the correlation and visualization of immunohistochemical results [23,24,25].

Statistical Analysis

IBM SPSS Statistics 21.0 (IBM Corp., Armonk, NY, USA) was used for all statistical analysis. The Student t-test, Mann-Whitney U test, chi-square test, or Fisher exact test was used to compare continuous and categorical variables. Values of p<0.05 were considered statistically significant. Receiver operating characteristic curve analysis was used to obtain cut-off values. The cut-off point values were calculated using the Youden index (Y = sensitivity + specificity - 1).

Table 1. Antibodies, sources, clones, pretreatments, and dilutions.

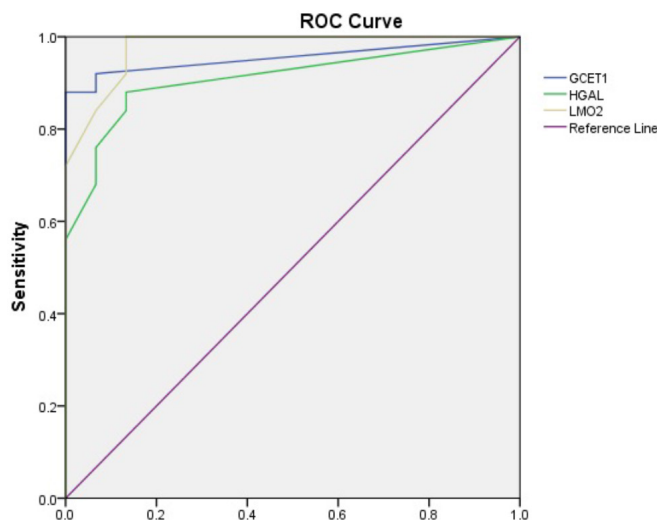| Antibody (Clone)	Source	Dilution	Retrieval	Incubation time/ temperature
GCET1 (RAM341)	Abcam	1/100	EDTA	120 min/37 °C
HGAL (MRQ-49)	Cell Marque	1/200	Citrate	120 min/37 °C
LMO2 (SP51)	Cell Marque	1/200	EDTA	120 min/37 °C

Figure 2. Receiver operating characteristic (ROC) curve showing the performances of GCET1, HGAL, and LMO2 in the separation of germinal center B-cell (GCB) and non-GCB phenotypes of Group A and B cases by immunohistochemistry.

Results

Control Group

Among the cases sampled in the control group, the patients' ages at the time of diagnosis ranged from 30 to 89 years, with a mean age of 53.8 years. The M/F ratio was 1, with 20 male and 20 female patients. Age and gender did not differ significantly between the low-grade and high-grade FL groups (p=0.447 and p=0.206, respectively). The FL infiltration pattern was follicular in 26 (65%) cases, focally follicular (predominantly diffuse) in 12 (30%) cases, and combined follicular and diffuse in 2 (5%) cases. There were no cases with a solely diffuse pattern.

CD10 was negative in 4 (10%) cases, which were all grade 3. There was no significant difference in the CD10 expressions of grade 1-2 and grade 3 cases (p=0.106). BCL6 was evaluated for 35 cases and was found to be positive in all of them.

The percentages of neoplastic cells positive for GCET1, HGAL, and LMO2 ranged from 0% to 100%, 0% to 100%, and 50% to 100% with medians of 80%, 70%, and 90%, respectively. GCET1, HGAL, and LMO2 staining did not differ significantly between grades (p=0.306, p=0.368, and p=0.343, respectively) or infiltration patterns (p=0.474, p=0.265, and p=0.778, respectively).

When the obtained cut-off values were applied to these cases, GCET1, HGAL, and LMO2 were positive in 34 (85%), 31 (77.5%), and 40 (100%) of the cases, respectively. All four cases that were negative for CD10 were positive for LMO2, and 3 of them were positive for GCET1 and HGAL. GCET1, HGAL, and LMO2 were found to have high sensitivity in all grades and infiltration patterns (Figure 3).

Among the cases of non-GC-derived NHL in the control group, GCET1, HGAL, and LMO2 were negative in all cases of ALCL, PTCL, SLL, and PBL (Figure 4). While GCET1 and HGAL were negative in all cases of MZL and MCL, LMO2 was positive in 2 of 3 MZL cases and 2 of 4 MCL cases. However, the expression was focal and/or weak in comparison to endothelial cells (Figure 4).

Diffuse Large B-cell Lymphoma

Among the cases of DLBCL included in this study, the mean age of the patients was 58 years (range: 17-82 years). Twenty-nine (44.6%) patients were female and 36 (55.4%) were male. Patients with the GCB phenotype were younger than those with the non-GCB phenotype, although the difference was not statistically significant (median age: 54 vs. 64 years, p=0.147).

Among the 65 DLBCL cases, 38 (58.4%) were classified as centroblast-dominant, 23 (35.3%) as immunoblast-dominant, and 4 (6.2%) as anaplastic. CD10 and BCL6 expressions were more common in the centroblast-dominant group, whereas MUM1 was expressed more commonly in the cases with immunoblast-dominant or anaplastic morphology (Table 2).

Among the Group A cases positive for CD10 and BCL6, 17 (85%) cases had a centroblast-dominant morphology (p=0.004). In contrast, the majority of the cases (12 of 15, 60%) in Group B had an immunoblast-dominant or anaplastic morphology. All Group C cases with BCL6 positivity and all but one of the triple-negative cases had a centroblast-dominant morphology. The morphology was heterogeneous in Group C cases showing BCL6 and MUM1 positivity, as 11 cases had an immunoblast-dominant

or anaplastic morphology and 9 cases had a centroblast-dominant morphology.

Among all considered DLBCL cases, GCET1, HGAL, and LMO2 positivity was observed in 23 (35.4%), 35 (53.8%), and 41 (63.1%) cases, respectively. Among the cases classified according to the Hans algorithm, GCET1, HGAL, and LMO2 were positive in 22 (88%), 21 (84%), and 25 (100%) of the GCB-DLBCL cases and 1 (2.5%), 14 (35%), and 16 (40%) of the non-GCB-DLBCL cases, respectively. The difference between GCB and non-GCB cases was statistically significant for each marker (p<0.001). The differences in the expressions of GCET1, HGAL, and LMO2 among morphological subgroups were also statistically significant (Table 2). The morphological and immunohistochemical features of the DLBCL cases are provided in the Supplemental Table.

A diagram tree was created using the hierarchical clustering method to analyze the immunoreactivity of CD10, BCL6, MUM1,

Table 2. Morphological findings for 65 cases of diffuse large B-cell lymphoma.

	Centroblast-dominant (n=38), n (%)	Immunoblast-dominant/anaplastic (n=27), n (%)	p
CD10	17 (44.7)	3 (11.1)	0.004
BCL6	31 (81.6)	14 (51.9)	0.01
MUM1	13 (34.2)	23 (85.2)	<0.001
GCET1	20 (52.6)	3 (11.1)	0.001
HGAL	30 (78.9)	5 (18.5)	<0.001
LMO2	32 (84.2)	9 (33.3)	<0.001

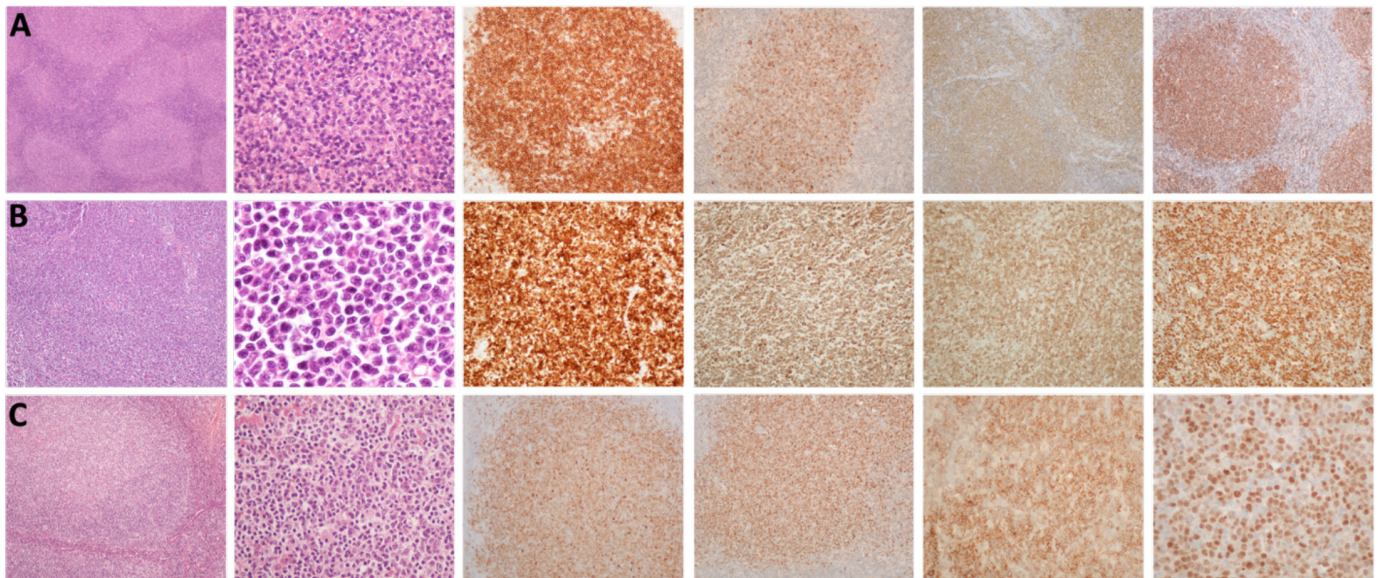**Figure 3.** Follicular lymphoma (FL): Hematoxylin and eosin (H&E)-stained sections of low-grade FL samples showing a follicular pattern (H&E, 40ˣ; H&E, 400ˣ) (A) and a diffuse pattern (H&E, 100ˣ; H&E, 1000ˣ) (B) consisting of predominantly centrocytic cells. H&E-stained sections of FL samples of grade 3 showing a follicular pattern and consisting of predominantly centroblastic cells (H&E, 100ˣ; H&E, 400ˣ) (C). CD10, GCET1, HGAL, and LMO2 positivity was observed in the neoplastic cells of FL samples (left to right, respectively; 200ˣ, 200ˣ, 100ˣ, and 100ˣ for A; 200ˣ for all in B; 100ˣ, 100ˣ, 200ˣ, and 400ˣ for C).
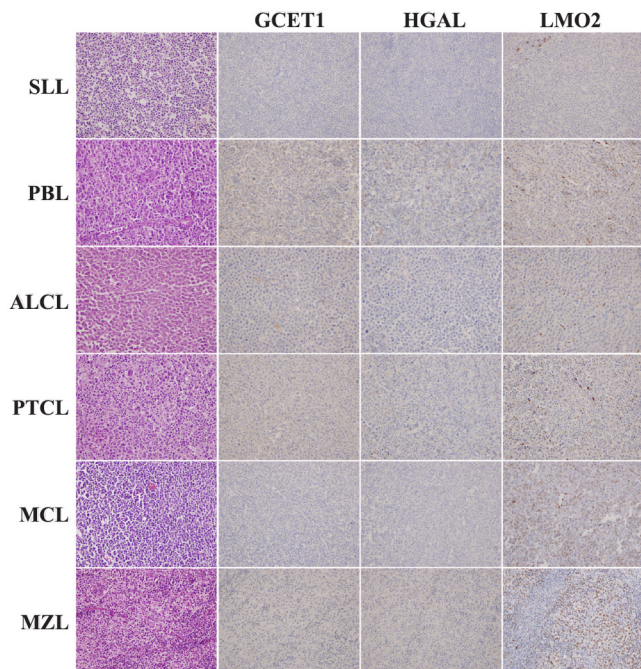
Figure 4. Histomorphology and GCET1, HGAL, and LMO2 immunoreactivity in non-germinal center-derived lymphomas (400ˣ for all). All three markers are negative in the cases of small lymphocytic lymphoma (SLL), plasmablastic lymphoma (PBL), anaplastic large-cell lymphoma (ALCL), and peripheral T-cell lymphoma (PTCL). Examples of GCET1 and HGAL negativity and LMO2 positivity in cases of marginal zone lymphoma (MZL) and mantle cell lymphoma (MCL) are given.

GCET1, HGAL, and LMO2 among the DLBCL cases (Figure 5). GCET1 clustered with CD10, while HGAL clustered with LMO2 and BCL6; they all formed a branch in the diagram associated with the GCB phenotype. The similarity was closest between the CD10 and GCET1 staining results. MUM1, associated with the non-GCB phenotype, formed a separate branch.

GCET1, HGAL, and LMO2 positivity was detected in 18 (90%), 17 (85%), and 20 (100%) of the 20 cases in Group A and in 0 (0%), 2 (13.3%), and 2 (13.3%) of the 15 cases in Group B, respectively (Figure 6). The differences in GCET1, HGAL, and LMO2 expressions between Groups A and B were statistically significant (p<0.001). The sensitivity, specificity, false negativity and false positivity, and positive and negative predictive values of GCET1, HGAL, and LMO2 in determining GCB phenotype alone or together are summarized in Table 3. HGAL had the highest false-positive rate and GCET1 had the lowest. When GCET1 and HGAL were used together, the sensitivity increased to 95% and the false-negative rate decreased to 0%. When all three antibodies were used together, the sensitivity increased to 100%, but the false-positive rate also increased (16.7%).

The intermediate group (Group C) included CD10-negative cases. Among the cases with positivity for only BCL6 (n=5), all but one
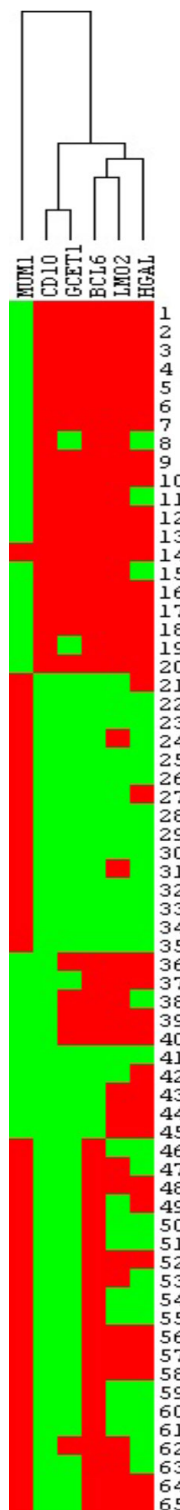
Figure 5. Hierarchical clustering analysis using immunohistochemical data in DLBCL cases. Positive staining is indicated as red and the lack of staining as green. The branching pattern of the dendrogram reflects similarities in the patterns of reactivity of the antibodies, with short branches denoting a high degree of similarity in expression patterns. HGAL clusters with LMO2 and BCL6, groups with GCET1 which clusters with CD10, associated with the GCB phenotype, on one branch of the dendrogram. MUM1 associated with the non-GCB phenotype, is on a separate branch.

Figure 6. Examples of DLBCL cases belonging to Group A and Group B and Group C. (A-D) Hematoxylin and eosin-stained sections showing centroblastic morphology in Group A (H&E, x1000) (A) and immunoblastic morphology in group B (H&E, x1000) (B) and cen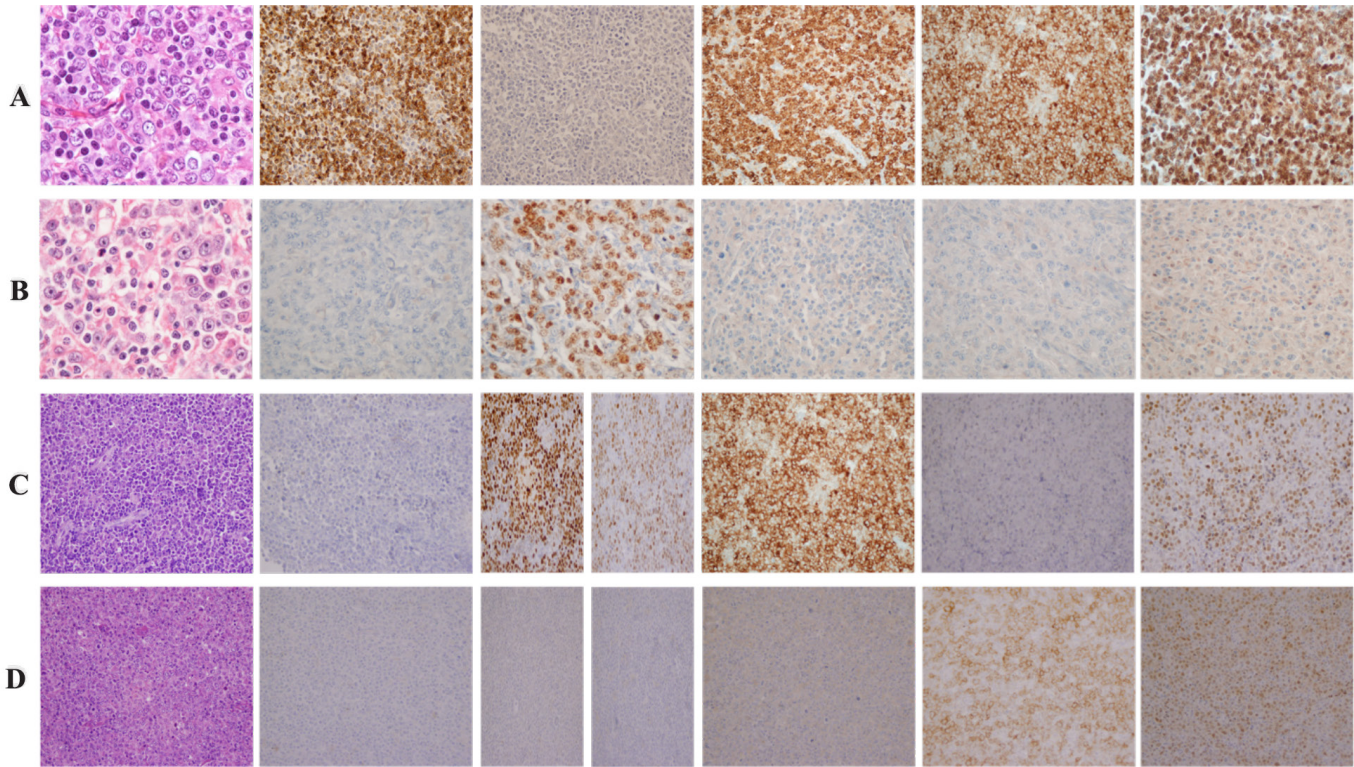troblastic morphology in group C (H&E, x400) (C-D). Immunohistochemical features: (A) CD10 positive (x200), MUM1 negative (x200), GCET1 (x200), HGAL (x200) and LMO2 (x400) positive (left to right, respectively), (B) CD10 negative, MUM1 positive, GCET1, HGAL and LMO2 negative (left to right, respectively) (x400 for all), (C) CD10 negative, BCL6 positive, MUM1 positive, GCET1 positive, HGAL negative, LMO2 positive (left to right, respectively) (x400 for all), (D) CD10, BCL6, MUM1 negative, GCET1 negative, HGAL, LMO2 positive (left to right, respectively) (x400 for all).

Table 3. Sensitivity, specificity, false negativity, false positivity, and positive and negative predictive values of GCET1, HGAL, and LMO2 in determining the germinal center B-cell phenotype alone or together.

	GCET1	HGAL	LMO2	GCET1 + HGAL	GCET1 + LMO2	HGAL + LMO2	GCET1 + HGAL + LMO2
Sensitivity (%)	90	85	100	95	100	100	100
Specificity (%)	100	86.7	86.7	86.7	86.7	73.3	73.3
False positivity (%)	0	10.5	9.1	9.5	9.1	16.7	16.7
False negativity (%)	12	18.8	0	7.1	0	0	0
Positive predictive power (%)	100	89.5	90.9	90.5	90.9	83.3	83.3
Negative predictive power (%)	88	81.3	100	92.9	100	100	100

were GCET1/HGAL-positive and all were LMO2-positive. They all had centroblast-dominant morphologies. Both morphological features and immunohistochemical findings supported the GCB phenotype, in line with the Hans algorithm. Triple-negative cases (n=5) were all negative for GCET1. Among them, only one case had an immunoblastic morphology and it was negative for all three considered markers. Therefore, this particular case was considered in the non-GCB group, in parallel with the Hans algorithm. The remaining four cases had centroblast-dominant

morphologies and showed HGAL and/or LMO2 immunoreactivity (Figure 6).

The 20 cases with both BCL6 and MUM1 positivity, which belonged to the non-GCB group according to the Hans algorithm, showed positivity for GCET1, HGAL, and LMO2 in 1 (5%), 8 (40%), and 11 (55%) cases, respectively. When the immunophenotypic and morphological features of this group were evaluated together, first of all, eight cases were found

to have immunoblast-dominant or anaplastic morphologies and these were all negative for GCET1, HGAL, and LMO2. Thus, in line with the Hans algorithm, these cases were considered in the non-GCB group. Second, three cases were positive only for LMO2. One of these had an anaplastic, one had an immunoblastic, and one had a centroblastic morphology. These findings were not found to be reliable for defining whether the cases belonged to the GCB or non-GCB group. Third, two cases had immunoblastic morphologies. Both were positive for HGAL and LMO2. Due to the high positive predictive value of the coexpression of HGAL and LMO2, they were considered to be in the GCB group, in contrast to the Hans classification. Fourth, six cases had centroblast-dominant morphologies. One of these cases was positive for only HGAL and the remaining were positive for both HGAL and LMO2. These cases were categorized within the GCB group, in contrast to the Hans classification. Finally, one case was positive for GCET1 and LMO2 and it had a centroblast-dominant morphology (Figure 6). Because of the specificity and high positive predictive value of GCET1, this case was thought to belong to the GCB group, in contrast to the Hans classification.

The findings of the GCET1, HGAL, and LMO2 results for the cases in Group C, the intermediate group, can be summarized as follows: First, these staining results were positive in CD10$^-$MUM$^-$BCL6$^+$ cases, supporting the GCB phenotype in line with the Hans algorithm. Second, nine of the 20 CD10$^-$BCL6$^+$MUM$^+$ cases, which belonged to the non-GCB group according to the Hans algorithm, were found to have the GCB phenotype. Third, four of the five CD10$^-$BCL6$^-$MUM$^-$ cases had centroblastic morphologies and were positive for GCET1, HGAL, and LMO2, supporting the GCB phenotype. Thus, when GCET1, HGAL, and LMO2 were applied as new GCB markers, a total of 13 cases that belonged to the non-GCB group according to the Hans algorithm were reclassified as having the GCB phenotype.

Discussion

DLBCL is a clinically and genetically heterogeneous disease that can be fully cured in fewer than half of all cases [26,27]. In GEP studies performed by cDNA microarray method, DLBCL cases were divided into the three different subgroups of GCB-like, ABC-like, and type 3 (unclassified) [4,5,7]. As patients with the GCB-like phenotype were found to have more favorable clinical courses independently of their IPI scores, the molecular distinction between the DLBCL subgroups became important [4,5]. Advances in targeted therapy have further increased the importance of accurate molecular classification. The nuclear factor kappa B (NF-κB) pathway is activated in ABC-DLBCL and represents a target for therapeutic strategies [28,29,30]. Recently new genetic classifications of DLBCL consisting of various genetic alterations and showing different outcomes were described [8,9,10,11,27]. Five distinct DLBCL subsets were discovered by genomic clustering, including an ABC/GCB-independent group with biallelic TP53 inactivation, CDKN2A loss, and associated genomic instability; two distinct subsets of GCB-DLBCLs with different outcomes and targetable alterations; and a previously unknown group of low-risk ABC-DLBCLs with extrafollicular/marginal zone origin [9,10]. In light of these studies, more targeted treatment options are sure to emerge in the future. Our understanding of high-grade B-cell lymphoma is still developing, but most cases of DLBCL-NOS broadly mirror the differentiation and maturation mechanisms active in normal B-cell development. Hence, the two main subtypes previously defined continue to be recognized, namely the GCB and non-GCB subtypes [26].

The aim of previous studies reported in the literature has been the accurate determination of the molecular subgroups of DLBCL cases by using immunohistochemistry, which is more feasible in routine clinical practice than GEP analysis [4,5,31]. The Hans algorithm was the first and remains the most widely used algorithm to investigate correlations between GEP results and antigen expression [12]. Although there is a good correlation with GEP in a majority of cases, some of the cases that are considered as non-GCB according to the Hans algorithm (e.g., triple-negative or CD10$^-$MUM1$^+$BCL6$^+$ cases) were found to be misclassified [12]. New algorithms including the GCET1 and LMO2 antibodies have been reported to have higher correlations with GEP results than the Hans algorithm [15,17,18].

GCET1 positivity in DLBCL ranges from 15% to 47% in the literature [18,32,33,34,35,36]. In the present study, GCET1 was found to be positive in 35.4% of cases, in accordance with the literature. Among the cases classified according to the Hans algorithm, 22 (88%) of 25 GCB cases and 1 (2.5%) of 40 non-GCB cases were positive for GCET1. In the study conducted by Montes-Moreno et al. [32], GCET1 positivity was found in 21 (68%) of 31 GCB cases and 3 (14%) of non-GCB cases, similar to the rates obtained in our study. Paterson et al. [33] reported that 47% of DLBCL cases were positive for GCET1, showing the highest concordance with CD10 in comparison to BCL6 and MUM1. In our study, GCET1 and CD10 showed the highest concordance in hierarchical clustering analysis, as reported in the literature.

HGAL expression in DLBCL was reported at rates of 28% to 74% in the literature [23,34,35,36]. In the study by Natkunam et al. [23], HGAL was positive in 68% of DLBCL cases, and overall, 61 (90%) of 68 GCB cases classified according to the Hans algorithm and 32 (47%) of the 68 non-GCB cases were positive for HGAL. In our study, HGAL was positive in 53.8% of DLBCL cases, including 21 (84%) of 25 GCB cases and 14 (35%) of 40 non-GCB cases. In both the literature and the present study, the high HGAL expression rates among cases with the non-GCB phenotype are striking findings.

LMO2 expression in DLBCL ranges between 15% and 82% in the literature [24,34,35,37]. Among cases classified according to the Hans algorithm, positive staining was reported in 61%-89% of GCB cases and 26%-50% of non-GCB cases [24,25,37]. In our study, LMO2 was positive in 63% of DLBCL cases, including 100% of cases in the GCB group and 40% of those in the non-GCB group, in line with the literature. LMO2 expression in the non-GCB group was high, similar to HGAL.

DLBCL has three morphological subgroups: centroblastic, immunoblastic, and anaplastic [38]. Non-GCB cases show immunoblastic morphologies (immunoblast ratio of >50%) more frequently than GCB cases. Furthermore, CD10-positive cases do not show immunoblastic morphologies [13]. In line with the literature, CD10-positive cases did not show immunoblastic morphologies in our study. In addition, an immunoblastic morphology was seen in 60% of the non-GCB cases while it was seen in only 12% of GCB cases. GCET1, HGAL, and LMO2 expression levels in cases of DLBCL with centroblastic morphology were significantly higher in comparison to cases with immunoblastic or anaplastic morphology, as expected.

Considering the reliability of CD10 and only MUM1 positivity in reflecting the GC and ABC phenotypes, respectively, we calculated the sensitivity and specificity of GCET1, HGAL, and LMO2 in determining the GCB phenotype among $CD10^+$ and $MUM1^+CD10^-BCL6^-$ cases. The remaining cases, which we considered together as the "intermediate group," were evaluated based on those results. Among them, 13 of 25 cases were considered to belong to the GCB group in contrast to the results of the Hans algorithm.

Among the 40 FL cases included in the present study, 34 (85%), 31 (77.5%), and 40 (100%) were positive for GCET1, HGAL, and LMO2, respectively. Four cases that were negative for CD10 were all positive for LMO2, and three of them were positive for GCET1 and HGAL. Our findings are in line with previous studies revealing the usefulness of these markers in reflecting the GC phenotype in CD10-negative FL cases [33,39,40,41,42]. Furthermore, GCET1 and HGAL were negative in the considered MZL, MCL, ALCL, PTCL, SLL, and PBL cases, which were non-GC-derived lymphomas, supporting their specificity in the determination of the GC phenotype. These findings are also in line with the literature [23,24,32,33,36]. LMO2 was negative in the ALCL, PTCL, SLL, and PBL cases, but some of the cases of MZL and MCL had focal/weak positivity. Both the literature and our findings show that LMO2 alone does not reflect the GC phenotype specifically and it should be used with other markers in the differential diagnosis of low-grade B-cell lymphomas [24,36].

In this study, GCET1, HGAL, and LMO2 were found to be useful in identifying the GC phenotype, and they also seem to be helpful in determining the GCB phenotype in cases showing the CD10⁻

$BCL6^+MUM1^+$ or triple-negative immunophenotype. The lack of confirmation of the molecular subtypes by GEP studies and the lack of clinical follow-up data are the limitations of our study. Hence, we cannot be certain about the additive effects of these markers in classifying the cell type of origin of DLBCL cases or their value in the risk stratification of patients. Nevertheless, the high expression levels of GCET1, HGAL, and LMO2 in the FL group and low or no expression in the non-GC-derived lymphoma group with cytomorphological correlations support our results.

Conclusion

GCET1, HGAL, and LMO2 are sensitive markers for the GC phenotype and morphology. In combination with the CD10, BCL6, and MUM1 panel, these markers increase the accuracy of the subclassification of DLBCL cases into prognostically different molecular subgroups and allow the accurate categorization of patients for targeted therapies.

Ethics

Ethics Committee Approval: This study's protocol was authorized by the Ethics Committee of the İstanbul Faculty of Medicine (file number: 64/2016).

Authorship Contributions

Concept- N.B., G.Y., Ö.D.; Design- N.B., G.Y., Ö.D.; Data Collection or Processing- N.B., G.Y., Y.Ö., Ö.D.; Analysis or Interpretation- N.B., G.Y., Y.Ö., Ö.D.; Literature Search- N.B.; Writing- N.B., G.Y., Y.Ö., Ö.D.

Conflict of Interest: No conflict of interest was declared by the authors.

References

1. [No authors listed.] A clinical evaluation of the International Lymphoma Study Group classification of non-Hodgkin's lymphoma. The Non-Hodgkin's Lymphoma Classification Project. Blood 1997;89:3909-3918.

2. Coiffier B. Diffuse large cell lymphoma. Curr Opin Oncol 2001;13:325-334.

3. The International Non-Hodgkin's Lymphoma Prognostic Factors Project. A predictive model for aggressive non-Hodgkin's Lymphoma. N Engl J Med 1993;329:987-994.

4. Alizadeh AA, Eisen MB, Davis RE, Ma C, Lossos IS, Rosenwald A, Boldrick JC, Sabet H, Tran T, Yu X, Powell JI, Yang L, Marti GE, Moore T, Hudson J Jr, Lu L, Lewis DB, Tibshirani R, Sherlock G, Chan WC, Greiner TC, Weisenburger

DD, Armitage JO, Warnke R, Levy R, Wilson W, Grever MR, Byrd JC, Botstein D, Brown PO, Staudt LM. Distinct types of diffuse large B-cell lymphoma identified by gene expression profiling. Nature 2000;403:503-511.

5. Rosenwald A, Wright G, Chan WC, Connors JM, Campo E, Fisher RI, Gascoyne RD, Muller-Hermelink HK, Smeland EB, Giltnane JM, Hurt EM, Zhao H, Averett L, Yang L, Wilson WH, Jaffe ES, Simon R, Klausner RD, Powell J, Duffey PL, Longo DL, Greiner TC, Weisenburger DD, Sanger WG, Dave BJ, Lynch JC, Vose J, Armitage JO, Montserrat E, López-Guillermo A, Grogan TM, Miller TP, LeBlanc M, Ott G, Kvaloy S, Delabie J, Holte H, Krajci P, Stokke T, Staudt LM; Lymphoma/Leukemia Molecular Profiling Project. The use of molecular profiling to predict survival after chemotherapy for diffuse large-B-cell lymphoma. N Engl J Med 2002;346:1937-1947.

6. Shipp MA, Ross KN, Tamayo P, Weng AP, Kutok JL, Aguiar RC, Gaasenbeek M, Angelo M, Reich M, Pinkus GS, Ray TS, Koval MA, Last KW, Norton A, Lister TA, Mesirov J, Neuberg DS, Lander ES, Aster JC, Golub TR. Diffuse large B-cell lymphoma outcome prediction by gene-expression profiling and supervised machine learning. Nat Med 2002;8:68-74.

7. Wright G, Tan B, Rosenwald A, Hurt EH, Wiestner A, Staudt LM. A gene expression-based method to diagnose clinically distinct subgroups of diffuse large B cell lymphoma. Proc Natl Acad Sci U S A 2003;100:9991-9916.

8. Wright GW, Huang DW, Phelan JD, Coulibaly ZA, Roulland S, Young RM, Wang JQ, Schmitz R, Morin RD, Tang J, Jiang A, Bagaev A, Plotnikova O, Kotlov N, Johnson CA, Wilson WH, Scott DW, Staudt LM. A probabilistic classification tool for genetic subtypes of diffuse large B cell lymphoma with therapeutic implications. Cancer Cell 2020;37:551-568.e14.

9. Chapuy B, Stewart C, Dunford AJ, Kim J, Kamburov A, Redd RA, Lawrence MS, Roemer MGM, Li AJ, Ziepert M, Staiger AM, Wala JA, Ducar MD, Leshchiner I, Rheinbay E, Taylor-Weiner A, Coughlin CA, Hess JM, Pedamallu CS, Livitz D, Rosebrock D, Rosenberg M, Tracy AA, Horn H, van Hummelen P, Feldman AL, Link BK, Novak AJ, Cerhan JR, Habermann TM, Siebert R, Rosenwald A, Thorner AR, Meyerson ML, Golub TR, Beroukhim R, Wulf GG, Ott G, Rodig SJ, Monti S, Neuberg DS, Loeffler M, Pfreundschuh M, Trümper L, Getz G, Shipp MA. Molecular subtypes of diffuse large B cell lymphoma are associated with distinct pathogenic mechanisms and outcomes. Nat Med 2018;24:679-690.

10. Wienand K, Chapuy B. Molecular classification of aggressive lymphomas—past, present, future. Hematol Oncol 2021;39(Suppl 1):24-30.

11. Schmitz R, Wright GW, Huang DW, Johnson CA, Phelan JD, Wang JQ, Roulland S, Kasbekar M, Young RM, Shaffer AL, Hodson DJ, Xiao W, Yu X, Yang Y, Zhao H, Xu W, Liu X, Zhou B, Du W, Chan WC, Jaffe ES, Gascoyne RD, Connors JM, Campo E, Lopez-Guillermo A, Rosenwald A, Ott G, Delabie J, Rimsza LM, Tay Kuang Wei K, Zelenetz AD, Leonard JP, Bartlett NL, Tran B, Shetty J, Zhao Y, Soppet DR, Pittaluga S, Wilson WH, Staudt LM. Genetics and pathogenesis of diffuse large B-cell lymphoma. N Engl J Med 2018;378:1396-1407.

12. Hans CP, Weisenburger DD, Greiner TC, Gascoyne RD, Delabie J, Ott G, Müller-Hermelink HK, Campo E, Braziel RM, Jaffe ES, Pan Z, Farinha P, Smith LM, Falini B, Banham AH, Rosenwald A, Staudt LM, Connors JM, Armitage JO, Chan WC. Confirmation of the molecular classification of diffuse large B-cell lymphoma by immunohistochemistry using a tissue microarray. Neoplasia 2004;103:275-282.

13. Colomo L, López-Guillermo A, Perales M, Rives S, Martínez A, Bosch F, Colomer D, Falini B, Montserrat E, Campo E. Clinical impact of the differentiation profile assessed by immunophenotyping in patients with diffuse large B-cell lymphoma. Blood 2003;101:78-84.

14. Muris JJ, Meijer CJ, Vos W, van Krieken JH, Jiwa NM, Ossenkoppele GJ, Oudejans JJ. Immunohistochemical profiling based on Bcl-2, CD10 and MUM1 expression improves risk stratification in patients with primary nodal diffuse large B cell lymphoma. J Pathol 2006;208:714-723.

15. Choi WW, Weisenburger DD, Greiner TC, Piris MA, Banham AH, Delabie J, Braziel RM, Geng H, Iqbal J, Lenz G, Vose JM, Hans CP, Fu K, Smith LM, Li M, Liu Z, Gascoyne RD, Rosenwald A, Ott G, Rimsza LM, Campo E, Jaffe ES, Jaye

DL, Staudt LM, Chan WC. A new immunostain algorithm classifies diffuse large B-cell lymphoma into molecular subtypes with high accuracy. Clin Cancer Res 2009;15:5494-5502.

16. Nyman H, Jerkeman M, Karjalainen-Lindsberg ML, Banham AH, Leppä S. Prognostic impact of activated B-cell focused classification in diffuse large B-cell lymphoma patients treated with R-CHOP. Mod Pathol 2009;22:1094-1101.

17. Meyer PN, Fu K, Greiner TC, Smith LM, Delabie J, Gascoyne RD, Ott G, Rosenwald A, Braziel RM, Campo E, Vose JM, Lenz G, Staudt LM, Chan WC, Weisenburger DD. Immunohistochemical methods for predicting cell of origin and survival in patients with diffuse large B-cell lymphoma treated with rituximab. J Clin Oncol 2011;29:200-207.

18. Visco C, Li Y, Xu-Monette ZY, Miranda RN, Green TM, Li Y, Tzankov A, Wen W, Liu WM, Kahl BS, d'Amore ES, Montes-Moreno S, Dybkær K, Chiu A, Tam W, Orazi A, Zu Y, Bhagat G, Winter JN, Wang HY, O'Neill S, Dunphy CH, Hsi ED, Zhao XF, Go RS, Choi WW, Zhou F, Czader M, Tong J, Zhao X, van Krieken JH, Huang Q, Ai W, Etzell J, Ponzoni M, Ferreri AJ, Piris MA, Møller MB, Bueso-Ramos CE, Medeiros LJ, Wu L, Young KH. Comprehensive gene expression profiling and immunohistochemical studies support application of immunophenotypic algorithm for molecular subtype classification in diffuse large B-cell lymphoma: a report from the International DLBCL Rituximab-CHOP Consortium Program Study. Leukemia 2012;26:2103-2113.

19. Lossos IS, Czerwinski DK, Alizadeh AA, Wechser MA, Tibshirani R, Botstein D, Levy R. Prediction of survival in diffuse large-B-cell lymphoma based on the expression of six genes. N Engl J Med 2004;350:1828-1837.

20. Lossos IS, Alizadeh AA, Rajapaksa R, Tibshirani R, Levy R. HGAL is a novel interleukin-4-inducible gene that strongly predicts survival in diffuse large B-cell lymphoma. System 2003;101:433-440.

21. Alaggio R, Amador C, Anagnostopoulos I, Attygalle AD, Araujo IBO, Berti E, Bhagat G, Borges AM, Boyer D, Calaminici M, Chadburn A, Chan JKC, Cheuk W, Chng WJ, Choi JK, Chuang SS, Coupland SE, Czader M, Dave SS, de Jong D, Du MQ, Elenitoba-Johnson KS, Ferry J, Geyer J, Gratzinger D, Guitart J, Gujral S, Harris M, Harrison CJ, Hartmann S, Hochhaus A, Jansen PM, Karube K, Kempf W, Khoury J, Kimura H, Klapper W, Kovach AE, Kumar S, Lazar AJ, Lazzi S, Leoncini L, Leung N, Leventaki V, Li XQ, Lim MS, Liu WP, Louissaint A Jr, Marcogliese A, Medeiros LJ, Michal M, Miranda RN, Mitteldorf C, Montes-Moreno S, Morice W, Nardi V, Naresh KN, Natkunam Y, Ng SB, Oschlies I, Ott G, Parrens M, Pulitzer M, Rajkumar SV, Rawstron AC, Rech K, Rosenwald A, Said J, Sarkozy C, Sayed S, Saygin C, Schuh A, Sewell W, Siebert R, Sohani AR, Tooze R, Traverse-Glehen A, Vega F, Vergier B, Wechalekar AD, Wood B, Xerri L, Xiao W. The 5th edition of the World Health Organization Classification of Haematolymphoid Tumours: Lymphoid Neoplasms. Leukemia 2022;36:1720-1748.

22. Eisen MB, Spellman PT, Brown PO, Botstein D. Cluster analysis and display of genome-wide expression patterns. Genetics 1998;95:14863-14868.

23. Natkunam Y, Lossos IS, Taidi B, Zhao S, Lu X, Ding F, Hammer AS, Marafioti T, Byrne GE Jr, Levy S, Warnke RA, Levy R. Expression of the human germinal center-associated lymphoma (HGAL) protein, a new marker of germinal center B-cell derivation. Blood 2005;105:3979-3986.

24. Natkunam Y, Zhao S, Mason DY, Chen J, Taidi B, Jones M, Hammer AS, Hamilton Dutoit S, Lossos IS, Levy R. The oncoprotein LMO2 is expressed in normal germinal-center B cells and in human B-cell lymphomas. Blood 2007;109:1636-1642.

25. Agostinelli C, Paterson JC, Gupta R, Righi S, Sandri F, Piccaluga PP, Bacci F, Sabattini E, Pileri SA, Marafioti T. Detection of LIM domain only 2 (LMO2) in normal human tissues and haematopoietic and non-haematopoietic tumours using a newly developed rabbit monoclonal antibody. Histopathology 2012;61:33-46.

26. Alaggio R, Amador C, Anagnostopoulos I, Attygalle AD, Araujo IBO, Berti E, Bhagat G, Borges AM, Boyer D, Calaminici M, Chadburn A, Chan JKC, Cheuk W, Chng WJ, Choi JK, Chuang SS, Coupland SE, Czader M, Dave SS,

de Jong D, Du MQ, Elenitoba-Johnson KS, Ferry J, Geyer J, Gratzinger D, Guitart J, Gujral S, Harris M, Harrison CJ, Hartmann S, Hochhaus A, Jansen PM, Karube K, Kempf W, Khoury J, Kimura H, Klapper W, Kovach AE, Kumar S, Lazar AJ, Lazzi S, Leoncini L, Leung N, Leventaki V, Li XQ, Lim MS, Liu WP, Louissaint A Jr, Marcogliese A, Medeiros LJ, Michal M, Miranda RN, Mitteldorf C, Montes-Moreno S, Morice W, Nardi V, Naresh KN, Natkunam Y, Ng SB, Oschlies I, Ott G, Parrens M, Pulitzer M, Rajkumar SV, Rawstron AC, Rech K, Rosenwald A, Said J, Sarkozy C, Sayed S, Saygin C, Schuh A, Sewell W, Siebert R, Sohani AR, Tooze R, Traverse-Glehen A, Vega F, Vergier B, Wechalekar AD, Wood B, Xerri L, Xiao W. World Health Organization Classification of Haematolymphoid Tumours, Fifth Edition: Lymphoid Neoplasms. Lyon, ICAR, 2022.

27. de Leval L, Alizadeh AA, Bergsagel PL, Campo E, Davies A, Dogan A, Fitzgibbon J, Horwitz SM, Melnick AM, Morice WG, Morin RD, Nadel B, Pileri SA, Rosenquist R, Rossi D, Salaverria I, Steidl C, Treon SP, Zelenetz AD, Advani RH, Allen CE, Ansell SM, Chan WC, Cook JR, Cook LB, d'Amore F, Dirnhofer S, Dreyling M, Dunleavy K, Feldman AL, Fend F, Gaulard P, Ghia P, Gribben JG, Hermine O, Hodson DJ, Hsi ED, Inghirami G, Jaffe ES, Karube K, Kataoka K, Klapper W, Kim WS, King RL, Ko YH, LaCasce AS, Lenz G, Martin-Subero JI, Piris MA, Pittaluga S, Pasqualucci L, Quintanilla-Martinez L, Rodig SJ, Rosenwald A, Salles GA, San-Miguel J, Savage KJ, Sehn LH, Semenzato G, Staudt LM, Swerdlow SH, Tam CS, Trotman J, Vose JM, Weigert O, Wilson WH, Winter JN, Wu CJ, Zinzani PL, Zucca E, Bagg A, Scott DW. Genomic profiling for clinical decision making in lymphoid neoplasms. Blood 2022;140:2193-2227.

28. Davis RE, Brown KD, Siebenlist U, Staudt LM. Constitutive nuclear factor κB activity is required for survival of activated B cell-like diffuse large B cell lymphoma cells. J Exp Med 2001;194:1861-1874.

29. Young RM, Schaffer ALI, Phelan JD, Staudt LM. B cell receptor signaling in diffuse large B cell lymphoma. Semin Hematol 2015;52:77-85.

30. Milhollen MA, Traore T, Adams-Duffy J, Thomas MP, Berger AJ, Dang L, Dick LR, Garnsey JJ, Koenig E, Langston SP, Manfredi M, Narayanan U, Rolfe M, Staudt LM, Soucy TA, Yu J, Zhang J, Bolen JB, Smith PG. MLN4924, a NEDD8-activating enzyme inhibitor, is active in diffuse large B-cell lymphoma models: rationale for treatment of NF-κB-dependent lymphoma. Blood 2010;116:1515-1523.

31. Lenz G, Wright GW, Emre NC, Kohlhammer H, Dave SS, Davis RE, Carty S, Lam LT, Shaffer AL, Xiao W, Powell J, Rosenwald A, Ott G, Muller-Hermelink HK, Gascoyne RD, Connors JM, Campo E, Jaffe ES, Delabie J, Smeland EB, Rimsza LM, Fisher RI, Weisenburger DD, Chan WC, Staudt LM. Molecular subtypes of diffuse large B-cell lymphoma arise by distinct genetic pathways. Proc Natl Acad Sci U S A 2008;105:13520-13525.

32. Montes-Moreno S, Roncador G, Maestre L, Martínez N, Sanchez-Verde L, Camacho FI, Cannata J, Martinez-Torrecuadrada JL, Shen Y, Chan WC, Piris MA. Gcet1 (centerin), a highly restricted marker for a subset of germinal center-derived lymphomas. Blood 2008;111:351-358.

33. Paterson MA, Hosking PS, Coughlin PB. Expression of the serpin centerin defines a germinal center phenotype in B-cell lymphomas. Am J Clin Pathol 2008;130:117-126.

34. Gutiérrez-García G, Cardesa-Salzmann T, Climent F, González-Barca E, Mercadal S, Mate JL, Sancho JM, Arenillas L, Serrano S, Escoda L, Martínez S, Valera A, Martínez A, Jares P, Pinyol M, García-Herrera A, Martínez-Trillos A, Giné E, Villamor N, Campo E, Colomo L, López-Guillermo A; Grup per l'Estudi dels Limfomes de Catalunya I Balears (GELCAB). Gene-expression profiling and not immunophenotypic algorithms predicts prognosis in patients with diffuse large B-cell lymphoma treated with immunochemotherapy. Blood 2011;117:4836-4843.

35. Gualco G, Bacchi LM, Domeny-Duarte P, Natkunam Y, Bacchi CE. The contribution of HGAL/GCET2 in immunohistological algorithms: a comparative study in 424 cases of nodal diffuse large B-cell lymphoma. Mod Pathol 2012;25:1439-1445.

36. Menter T, Gasser A, Juskevicius D, Dirnhofer S, Tzankov A. Diagnostic utility of the germinal center-associated markers GCET1, HGAL, and LMO2 in hematolymphoid neoplasms. Appl Immunohistochem Mol Morphol 2015;23:491-498.

37. Morton LM, Cerhan JR, Hartge P, Vasef MA, Neppalli VT, Natkunam Y, Dogan A, Dave BJ, Jain S, Levy R, Lossos IS, Cozen W, Davis S, Schenk MJ, Maurer MJ, Lynch CF, Rothman N, Chatterjee N, Yu K, Staudt LM, Weisenburger DD, Wang SS. Immunostaining to identify molecular subtypes of diffuse large B-cell lymphoma in a population-based epidemiologic study in the pre-rituximab era. Int J Mol Epidemiol Genet 2011;2:245-252.

38. Swerdlow SH, Campo E, Pileri SA, Harris NL, Stein H, Siebert R, Advani R, Ghielmini M, Salles GA, Zelenetz AD, Jaffe ES. The 2016 revision of the World Health Organization classification of lymphoid neoplasms. Blood 2016;127:2375-2390.

39. Goteri G, Lucarini G, Zizzi A, Costagliola A, Giantomassi F, Stramazzotti D, Rubini C, Leoni P. Comparison of germinal center markers CD10, BCL6 and human germinal center-associated lymphoma (HGAL) in follicular lymphomas. Diagn Pathol 2011;6:97.

40. Younes SF, Beck AH, Lossos IS, Levy R, Warnke RA, Natkunam Y. Immunoarchitectural patterns in follicular lymphoma: efficacy of HGAL and LMO2 in the detection of the interfollicular and diffuse components. Am J Surg Pathol 2010;34:1266-1276.

41. Younes SF, Beck AH, Ohgami RS, Lossos IS, Levy R, Warnke RA, Natkunam Y. The efficacy of HGAL and LMO2 in the separation of lymphomas derived from small B cells in nodal and extranodal sites, including the bone marrow. Am J Clin Pathol 2011;135:697-708.

42. Weinberg OK, Ma L, Seo K, Beck AH, Pai RK, Morales A, Kim Y, Sundram U, Tan D, Horning SJ, Hoppe RT, Natkunam Y, Arber DA. Low stage follicular lymphoma: biologic and clinical characterization according to nodal or extranodal primary origin. Am J Surg Pathol 2009;33:591-598.

Supplement Table 1. Morphological/immunohistochemical features of DLBCL cases.

	No	Morphology	Hans algorithm	GCET1	HGAL	LMO2
Group A CD10(+) BCL6(+) MUM1(-) or(+)	1	CB	GCB	+	+	+
	2	CB		+	+	+
	3	CB		+	+	+
	4	CB		+	+	+
	5	CB		+	+	+
	6	CB		+	+	+
	7	IB		+	+	+
	8	CB		-	-	+
	9	IB		+	+	+
	10	CB		+	+	+
	11	IB		+	-	+
	12	CB		+	+	+
	13	CB		+	+	+
	14	CB		+	+	+
	15	CB		+	-	+
	16	CB		+	+	+
	17	CB		+	+	+
	18	CB		+	+	+
	19	CB		-	+	+
	20	CB		+	+	+
Group B CD10(-) BCL6(-) MUM1(+)	1	CB	Non-GCB	-	+	-
	2	IB		-	-	-
	3	CB		-	-	-
	4	AP		-	-	+
	5	IB		-	-	-
	6	IB		-	-	-
	7	IB		-	+	-
	8	AP		-	-	-
	9	IB		-	-	-
	10	IB		-	-	-
	11	IB		-	-	+
	12	CB		-	-	-
	13	IB		-	-	-
	14	IB		-	-	-
	15	IB		-	-	-
Group C CD10(-) BCL6(+) MUM1(-)	1	CB	GCB	+	+	+
	2	CB		-	+	+
	3	CB		+	-	+
	4	CB		+	+	+
	5	CB		+	+	+

Supplement Table 1. Continued						
	No	Morphology	Hans algorithm	GCET1	HGAL	LMO2
Group C CD10^{-} BCL6^{+} MUM1^{+}	1	IB	Non-GCB	–	–	–
	2	AP		–	–	+
	3	IB		–	+	+
	4	CB		–	+	–
	5	CB		–	–	–
	6	AP		–	–	–
	7	IB		–	+	+
	8	IB		–	–	+
	9	IB		–	–	–
	10	IB		–	–	–
	11	CB		–	+	+
	12	CB		–	+	+
	13	CB		–	+	+
	14	IB		–	–	–
	15	IB		–	–	–
	16	IB		–	–	–
	17	CB		+	–	+
	18	CB		–	–	+
	19	CB		–	+	+
	20	CB		–	+	+
Group C CD10^{-} BCL6^{-} MUM1^{-}	1	IB	Non-GCB	–	–	–
	2	CB		–	+	–
	3	CB		–	+	+
	4	CB		–	+	+
	5	CB		–	+	+
CB: Centroblastic, IB: immunoblastic, AP: anaplastic, GCB: germinal center B						